UNDERSTANDING NEAR-SURFACE AND IN-CLOUD TURBULENT FLUXES IN THE COASTAL STRATOCUMULUS-TOPPED BOUNDARY LAYERS

FINAL TECHNICAL REPORT

BY

IOANNIS KALOGIROS

OCTOBER 2004

NAVAL POSTGRADUATE SCHOOL, CA, USA

CONTRACT NUMBER   N62558-03-M-0043

NATIONAL OBSERVATORY OF ATHENS, ATHENS, GREECE

APPROVED FOR PUBLIC RELEASE; DISTRIBUTION UNLIMITED

REPORT DOCUMENTATION PAGE

Form Approved
OMB No. 0704-0188

1. REPORT DATE *(DD-MM-YYYY)*	2. REPORT TYPE	3. DATES COVERED *(From - To)*
30-10-2004	Final Report	August 2003-August 2004

4. TITLE AND SUBTITLE	5a. CONTRACT NUMBER
Understanding Near-surface and In-cloud Turbulent Fluxes in the Coastal Stratocumulus-topped Boundary	N62558-03-M-0043

5b. GRANT NUMBER

5c. PROGRAM ELEMENT NUMBER

6. AUTHOR(S)

Ioannis A. Kalogiros

5d. PROJECT NUMBER

5e. TASK NUMBER

5f. WORK UNIT NUMBER
004

7. PERFORMING ORGANIZATION NAME(S) AND ADDRESS(ES)

National Observatory of Athens,
Athens, 11810, Greece

8. PERFORMING ORGANIZATION REPORT NUMBER

9. SPONSORING/MONITORING AGENCY NAME(S) AND ADDRESS(ES)

Naval Postgraduate School,
Monterey, CA 93943, USA

10. SPONSOR/MONITOR'S ACRONYM(S)

11. SPONSORING/MONITORING AGENCY REPORT NUMBER

12. DISTRIBUTION AVAILABILITY STATEMENT
Approved for Public Release; distribution unlimited.

13. SUPPLEMENTARY NOTES
Any opinions, findings and conclusions or recommendations expressed in this material are those of the author(s) and do not necessarily reflect the views of the Naval Postgraduate School or the U.S. Government.

14. ABSTRACT

Aircraft data collected in Monterey Bay area from forty flights in the framework of Autonomous Ocean Sampling Network (AOSN-II) project were used to study the spatial variability and bulk parameterization of turbulence surface fluxes in a coastal region. Flight maneuvers were used to calibrate the turbulence wind data obtained from a radome probe. The typical flight pattern consisted of dense near sea surface straight legs. A variety of near surface flow patterns with downcoast and upcoast strong or weak flow as well as offshore flow was observed. The wind field was quite complex due to intense topographical effects like flow channeling and thermal flows. In addition, coastal upwelling and stratocumulus cloud contribute significantly in the complexity of the atmospheric flow in the measurements area. Measured surface turbulent fluxes were found to be systematically lower than bulk estimations. Non-homogeneity of the flow, limited validity of surface similarity functions, low level clouds effects and poor roughness length parameterization especially under stable atmospheric conditions in the coastal area are probable reasons for this deviation.

15. SUBJECT TERMS
Coastal area, Turbulence Fluxes, Spatial Variability, Bulk Parameterization

16. SECURITY CLASSIFICATION OF:			17. LIMITATION OF ABSTRACT	18. NUMBER OF PAGES	19a. NAME OF RESPONSIBLE PERSON
a. REPORT	b. ABSTRACT	c. THIS PAGE			Ioannis Kalogiros
Unclassified	Unclassified	Unclassified	UU	24	19b. TELEPHONE NUMBER *(Include area code)* +30 210 8109135

Standard Form 298 (Rev. 8-98)
Prescribed by ANSI-Std Z39-18

THIS PAGE INTENTIONALLY LEFT BLANK

ABSTRACT

Aircraft data collected in Monterey Bay area from forty flights in the framework of Autonomous Ocean Sampling Network (AOSN-II) project were used to study the spatial variability and bulk parameterization of turbulence surface fluxes in a coastal region. Flight maneuvers were used to calibrate the turbulence wind data obtained from a radome probe. The typical flight pattern consisted of dense near sea surface straight legs. A variety of near surface flow patterns with downcoast and upcoast strong or weak flow as well as offshore flow was observed. The wind field was quite complex due to intense topographical effects like flow channeling and thermal flows. In addition, coastal upwelling and stratocumulus cloud contribute significantly in the complexity of the atmospheric flow in the measurements area. Measured surface turbulent fluxes were found to be systematically lower than bulk estimations. Non-homogeneity of the flow, limited validity of surface similarity functions, low level clouds and poor roughness length parameterization especially under stable atmospheric conditions in the coastal area are probable reasons for this deviation.

KEYWORDS

THIS PAGE INTENTIONALLY LEFT BLANK

TABLE OF CONTENTS

THIS PAGE INTENTIONALLY LEFT BLANK

1. INTRODUCTION

The air-sea exchange of water vapor, heat, and momentum is important in many scales of atmospheric and oceanic motions. A critical issue in numerical atmospheric models is the determination of lower boundary conditions. In order to predict correctly the boundary layer evolution in a complex and relatively poorly understood environment like coastal areas better understanding of the spatial variability and more accurate parameterization of turbulence surface fluxes are needed.

In the area of measurements (Monterey Bay, California) used in this study intense topographical effects like flow channeling due to coastal topography and thermal flows between land and sea in combination with stratocumulus cloud and coastal upwelling contribute to the complexity of the wind flow near the coast. The Rossby radius of deformation, which is a measure of the offshore distance of influence of coastal effects, is about 100 km and, thus, it covers a significant area. Two significant characteristics of the marine boundary layer off the California coast are the stratocumulus clouds and the low-level coastal wind jet. The variable wind stress field near the coast forces local upwelling of cold water through Ekman pumping [1]. The cold sea surface temperatures near the coast due to upwelling and the strong temperature inversion at the top of the boundary layer due the synoptic scale subsidence favor the development of stratocumulus cloud during the summer. The enhanced turbulent mixing in the cloud layer may affect near surface turbulence, especially in conditions where the height of cloud top is small as it is the case near California coast. The coastal wind jet is mainly the result of the large horizontal temperature gradient (baroclinity) between the cold air above the sea and the warm air above land (thermal wind) and the frictional effect within the atmospheric boundary layer [2,3]. Topographical features may intensify this wind jet at significant convex bends of the coastline like Cape Mendocino, Pt. Arena and Pt. Sur. At such changes of the coastline geometry combined with mountain barriers (channeling effect) the northerly flow can become supercritical. An expansion fan occurs at the bend and a strong wind jet evolves downstream of the bend with significant lowering of the boundary layer top [4]. Also, thermally induced local flows like the sea breeze are observed in the measurements area with significant offshore extent [5]. In this non-homogeneous coastal environment advective and sea surface wave effects are expected to be significant and common assumptions like similarity theory in the atmospheric surface layer may not be valid. Thus, bulk parameterizations of turbulence surface fluxes that are based on similarity theory [6,7] may fail especially under stable atmospheric conditions [8,9,10,11].

Aircraft measurements can resolve the spatial variability in coastal areas with carefully designed flight patterns which cannot be done with the usually limited coastal stations and buoys routine measurements. In this work we use aircraft data from dense flight legs close to the sea surface in order to study the spatial variability of surface turbulent fluxes and the validity of bulk parameterization schemes in a coastal region. First, we show case studies of commonly observed flow and turbulence spatial patterns that reveal the coastal effect under various forcing. Next, we show that bulk parameterizations systematically overestimate turbulence surface fluxes significantly under stable atmospheric conditions and there is large scatter from expected behavior of bulk transfer coefficients.

2. MEASUREMENTS AND DATA PROCESSING

High-rate 10 Hz measurements of turbulence were obtained with the CIRPAS/NPS Twin Otter aircraft in Monterey Bay throughout the year 2003 in the framework of Autonomous Ocean Sampling Network (AOSN-II) project. Data include about forty flights which were carried out from morning to early afternoon of each day. In some days with low winds the local sea breeze in Monterey Bay area was developing and, thus, a significant change of atmospheric state (especially wind flow) was observed during the passage of the aircraft from the same area during the flight. The usual flight pattern consisted of dense near sea surface (30-40 m above sea surface) straight legs and some slant soundings north and south of the coverage area from 36° to 37° latitude within 100 km from the coastline. Wind turbulence was estimated from a radome five holes pressure probe and GPS (aircraft position, velocity and attitude angles) data after a careful calibration using flight maneuvers [12]. Fast temperature and humidity measurements were obtained with a Rosemount platinum resistance thermometer and an IRGA sensor, respectively. A second order polynomial calibration of IRGA fast humidity sensor against a dew point hygrometer was achieved using a filter method that effectively separated the slow drifting voltage offset that IRGA sensors suffer from faster variations.

Turbulence quantities like momentum, sensible heat, and latent heat fluxes were calculated with the eddy correlation method and a horizontal averaging length of 5 km. Ogive (cumulative co-spectrum) analysis showed that this averaging length is sufficient and includes all the energy containing scales. We note that the height of marine boundary layer (MABL) close to the California coast is usually less than 500-600 m and surface fluxes (thus, turbulence energy lies in small scales) are analyzed. In addition to turbulent fluxes, the divergence and curl of wind and wind stress was estimated after an interpolation of surface momentum fluxes to a regular grid with 5 km spacing. Peak values of wind stress curl are expected to be connected with regions of enhanced upwelling near the coast. After a quality control of all available data a total of 3695 flux measurements with most of stability z/L values (L is the Monin-Obukhov length) ranging in the range -2 to 0.2 was obtained. Wind stress was calculated from $\tau=\rho(<w'u'>^2+<w'v'>^2)^{1/2}=\rho u_*^2$ and sensible and latent heat fluxes from $H_s=\rho C_p<w'\theta'>$ and $H_l=\rho L_v<w'r'>$, respectively, where u, v, and w are the wind east, north and vertical components, respectively, ρ is air density, u_* is the friction velocity, C_p is the specific heat of air, L_v is the latent heat of vaporization of water, θ is air potential temperature, r is the water vapor mixing ratio. The <> symbols indicate time average and the primes indicate variations from average quantities. Transfer coefficients C_d, C_h, and C_e for momentum, sensible heat, and latent heat (water vapor) flux were calculated from $\tau=\rho C_d SU$, $H_s=\rho C_p C_h S(\theta_s-\theta)$, and $H_l=\rho L_v C_e S(r_s-r)$. Sea surface temperature T_s (θ_s is the corresponding potential temperature) was measured with a radiative thermometer and r_s at sea surface was estimated by T_s and air static pressure at sea surface P_s including the about 2% salinity effect. The parameter S includes the gustiness factor in addition to vector averaged wind speed $U=(<u>^2+<v>^2)^{1/2}$ and average bulk quantities were reduced to a common reference height of 10 m using the flux-profile functions of [7]. Bulk estimates of τ, H_s, H_l, C_d, C_h, and C_e were obtained with widely used COARE version 3.0 algorithm [7]. Transfer coefficients were reduced to neutral conditions of atmospheric stability using the same flux-profile relations with an iterative method which incorporates the difference between roughness length at measurement conditions and neutral stability [6].

3. SPATIAL VARIABILITY

3.1. Downcoast flow

The typical wind flow conditions, especially during summer, at the California coast is a north wind parallel to the coast that is intensified offshore. This flow pattern is due to the persistent high pressure system of Pacific Ocean. Due to the complexity of the coastal mountain barriers and the small MABL height because of large scale subsidence and coastal upwelling, flow channeling and hydraulic like phenomena (expansion fans) are usually observed at the Capes and Points. Such observations were included in the AOSN-II data set, too, at the Pescadero and Big Sur Points north and south, respectively, of Monterey Bay. The significant boundary layer height change (which is characteristic of these phenomena) at these Points was not observed directly because the flight pattern did not include many soundings, but the local intensification of wind speed and the surface pressure pattern are very good indicators. However, the contribution of other effects like lee waves in the observations is not excluded and it is actually difficult to separate flow channeling from lee wave effects in observations.

Figure 1 shows surface plots of various quantities observed at the north part of Monterey Bay while Fig. 2 shows the large scale synoptic conditions (the 850 hPa level corresponds to geostrophic flow abound the boundary layer at least offshore) on such a case on July 13, 2003. An area of higher wind and wind direction turning is clear at the north of Monterey Bay connected with a low surface pressure area. The depression of about 2 hPa indicates a lowering of the MABL height by about 200 m in that area. Wind divergence field (connected to vertical velocity through continuity, not shown here) and the negative sensible heat flux area due to the heating of air by subsidence agree with such a behavior too. The air heating can also be the result of a lee wave disturbance. The hydraulic theory explanation of the flow pattern does not include such an effect. The wind stress and vertical velocity variance is higher at the high wind zone but quite in respect to the 15-20 ms^{-1} wind values in this area. The peak of wind stress curl is about in place with the colder sea surface temperature area in this case but smaller than peak values of 4×10^{-5} ms^{-2} from past observations in more significant Capes of the coast like Cape Mendocino or Pt. Arena to the north [1,8]. Under downcoast flow the above described pattern was common but it seems
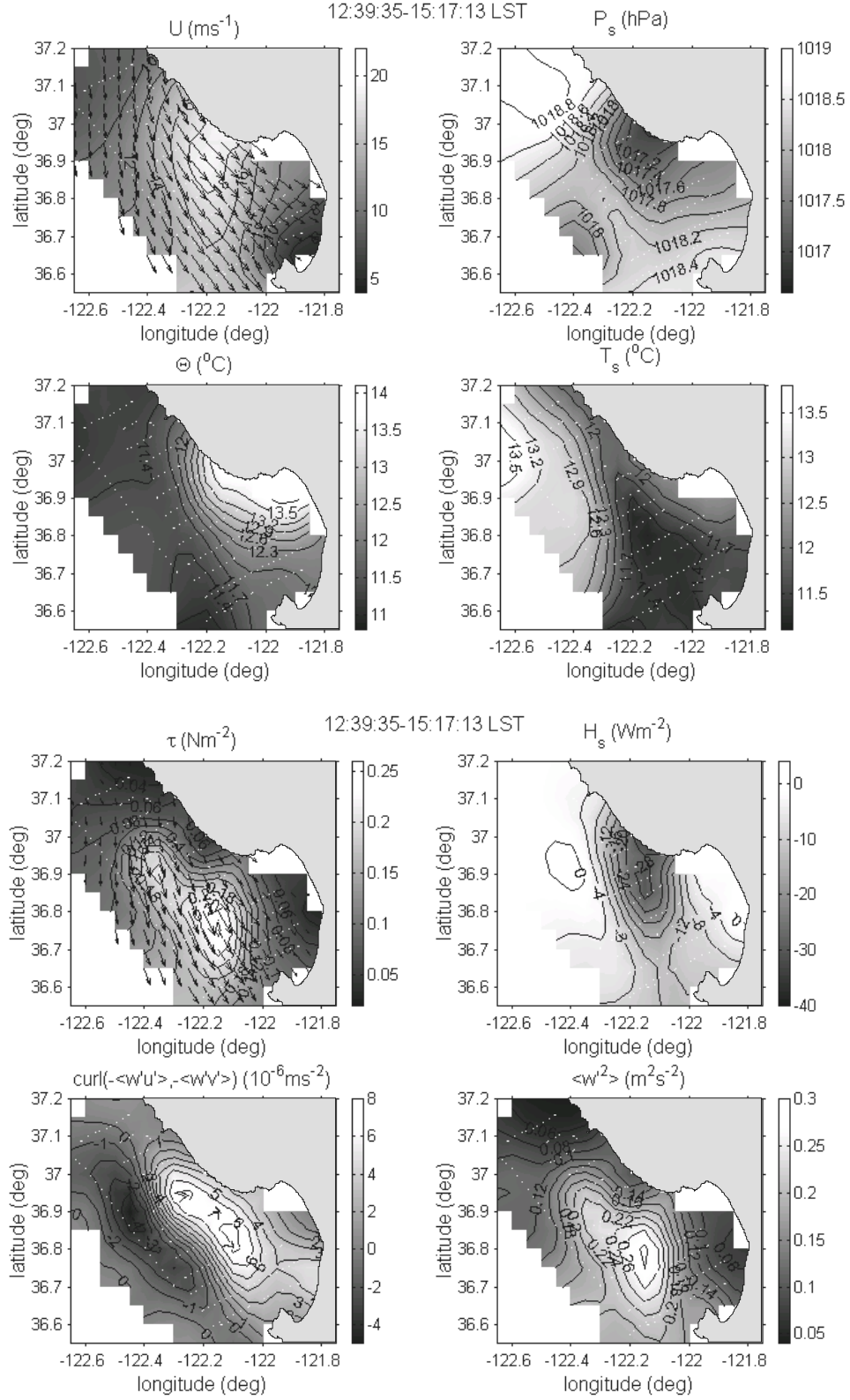
FIG. 1. Mean and turbulence quantities near sea surface on 13 July 2003. The flight pattern is shown with white dots.
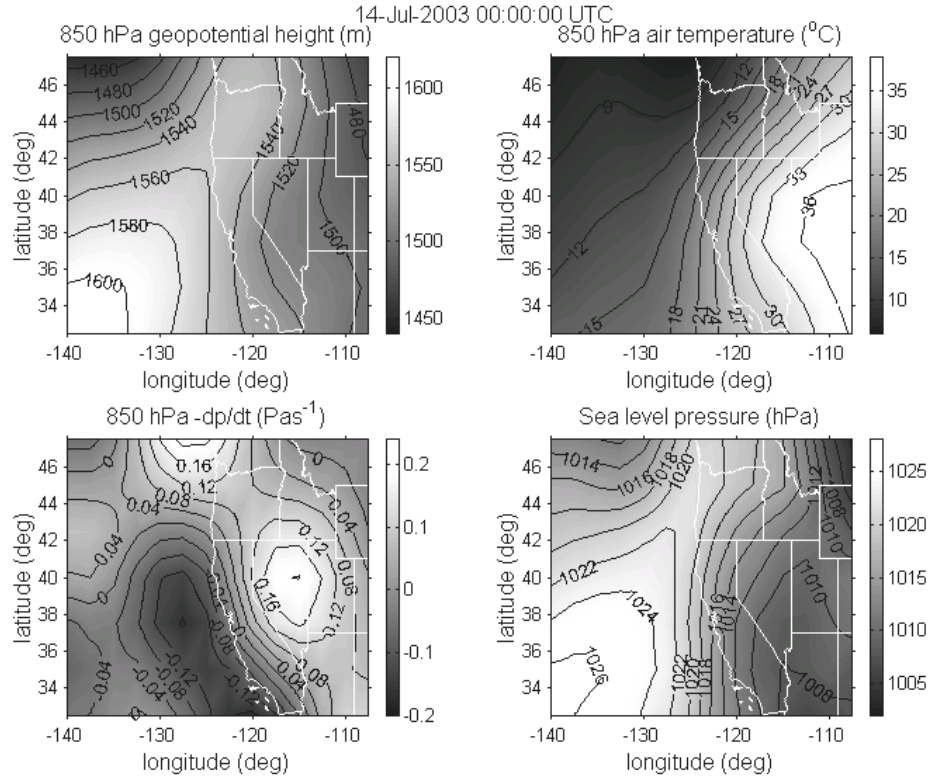
FIG. 2. Synoptic conditions on 13 July 2003 from NCEP/NCAR reanalysis data provided by the NOAA-CIRES Climate Diagnostics Center.

that a slight variation of the synoptic wind direction and strength and large scale subsidence could result either in no development of that pattern or a similar pattern to develop just south of Pt. Sur. Synoptic conditions in favor of such a flow channeling are a significant horizontal gradient of sea surface pressure which gives strong north sector winds parallel to the coast or with a small onshore component and a large scale subsidence zone (like the one that occurs at the west part of a trough) just offshore the measurement area which gives small MABL depth (see Fig. 2). In any case, however, a significant characteristic of such flow pattern was that turbulence level was low for such high winds.

3.2 Onshore flow

Under low large scale wind flow local thermal flows may be well developed in Monterey Bay. Figures 3 and 4 show such a case, where a zone of onshore light flow (probably a sea breeze) parallel to the coast has been developed in the morning and is separated by further offshore flow by a divergence (implying local subsidence) and high pressure zone. A noticeable feature is that turbulent fluxes are very low at that time period especially in Monterey Bay. Another characteristic on this day is that the intensity of upwelling coastal zone is probably reduced and, thus, the sea surface temperature is high (17°C) and the near surface air temperature is very close to sea surface temperature. The synoptic conditions show that there is weak extended trough over the west coast with its axis parallel to the coastline. Thus, there is a weak onshore wind flow above the boundary layer as well as a weak large scale flow from the north sector with onshore component near the surface (see Fig. 4).

We note that under low winds there were also a couple of cases with southern surges close to the coast that just reach Monterey Bay like the case shown in Fig. 5. The synoptic conditions (not shown here) were a cold anticyclone (winter time) over middle-west US and, most importantly, a very weak horizontal gradient of sea surface pressure over southern California. Unfortunately, the lack of enough soundings in the flight patterns does not permit the identification of the vertical structure of such flow surges.
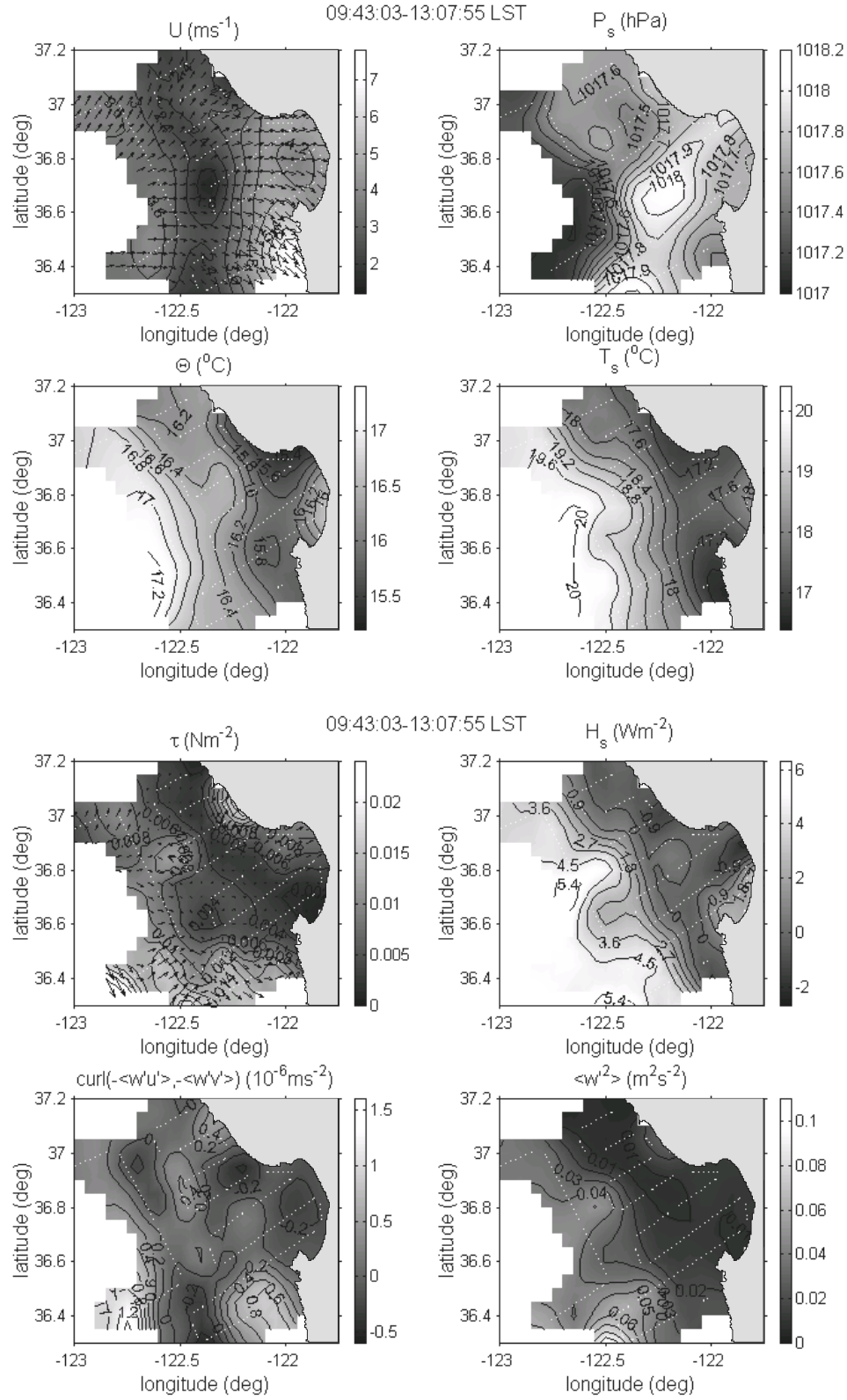
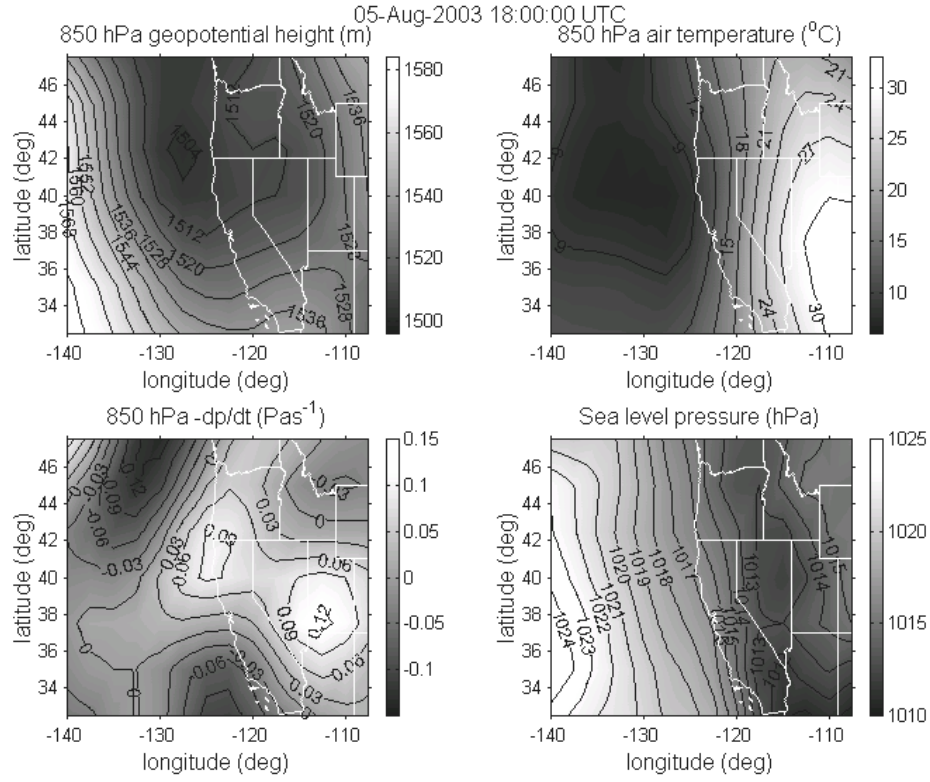FIG. 3. Same as Fig. 1 but for 5 August 2003.

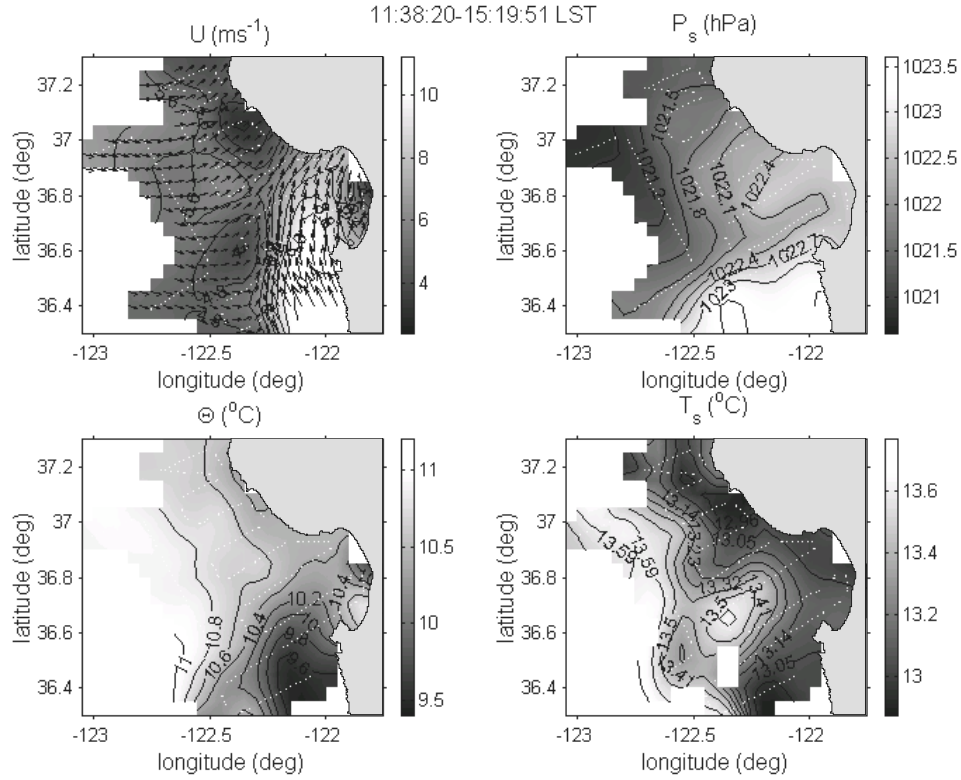FIG. 4. Same as Fig. 2 but for 5 August 2003.

FIG. 5. Mean quantities near sea surface on 27 January 2004. The flight pattern is shown with white dots.
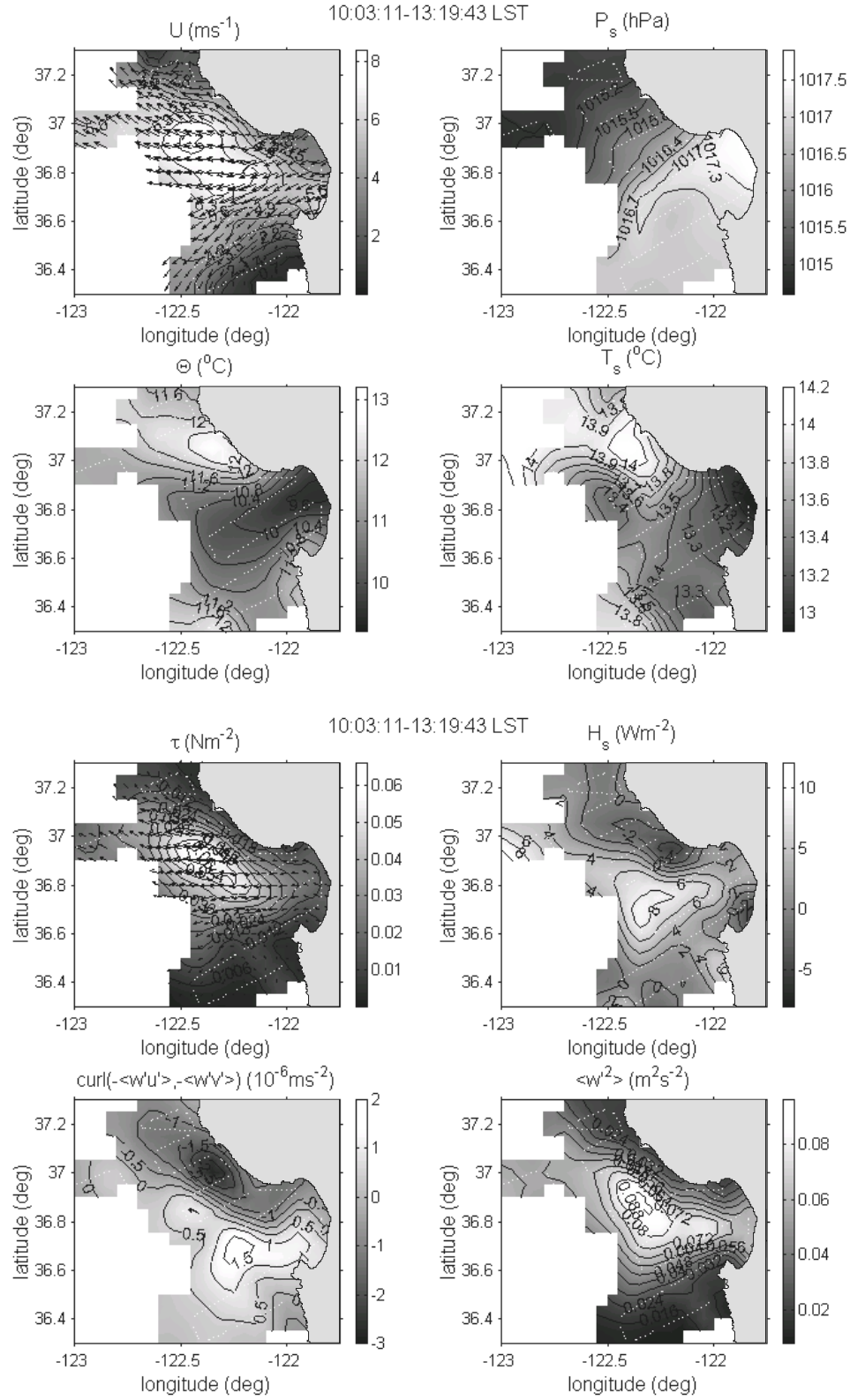
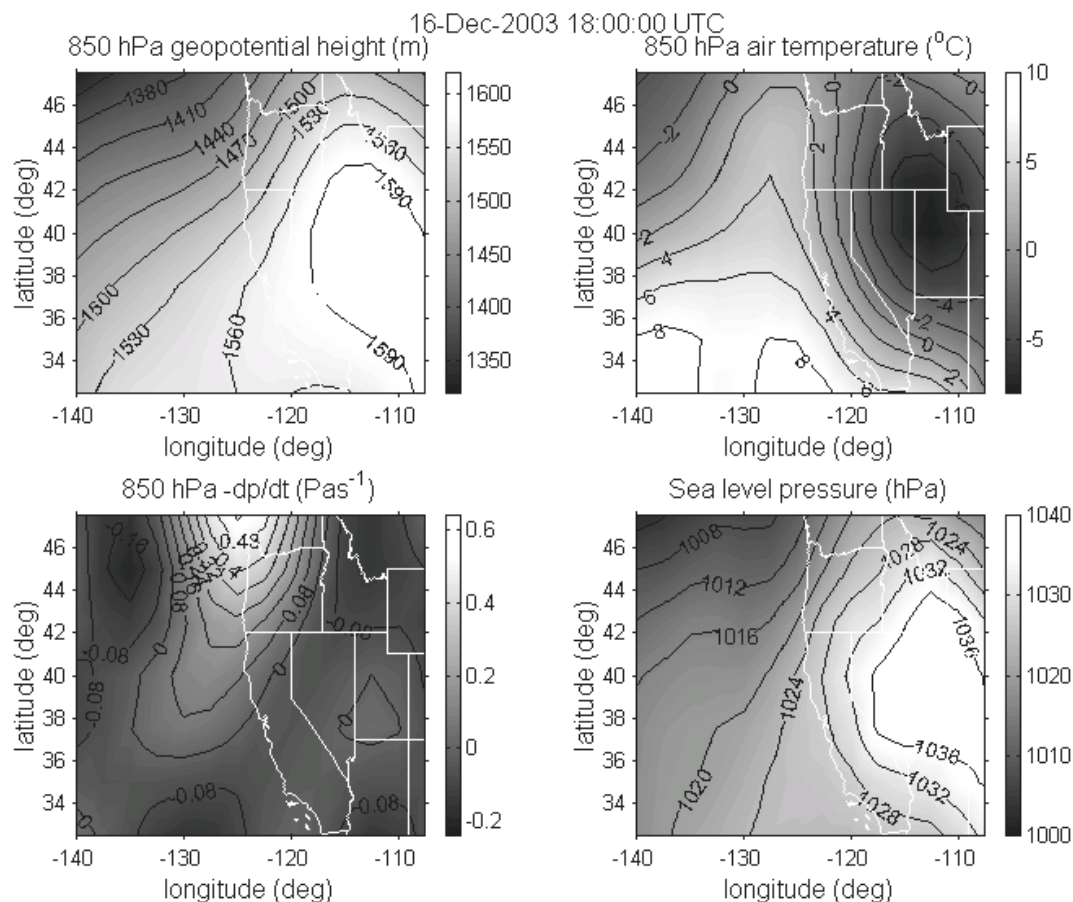FIG. 6. Same as Fig. 1 but for 16 December 2003.

FIG. 7. Same as Fig. 2 but for 16 December 2003.

3.3 Offshore flow

When the usual north flow was low or not existing an outflow from Monterey was also observed in some cases. Figures 6 and 7 show the observations from such a case. The cold outflow from Salinas Valley intensifies and diverges as it comes out over the Monterey Bay. The synoptic condition that gave this near surface flow pattern is a cold anticyclone over the west US (Fig. 7) during winter time. The increased (but still low compared to downcoast winds cases) turbulence level offshore affects the sea surface temperature pattern through the wind stress effect on upwelling.

Finally, cases with southern (upcoast) flow in the whole observation area were also included in the data set (not shown here) and were characterized by low turbulence and a limited upwelling zone as it is expected from the southern wind stress direction that gives an onshore sea surface current. The synoptic condition that gave upcoast flow near the surface was either a low pressure system off the California coast during the summer, which is probably a trapped disturbance after an extension of the thermal low pressures from the west US towards offshore [13], like in the time period 20-22 August 2003 (not shown here) or a low pressure weather system approaching from the west during winter.

4. BULK PARAMETERIZATION

4.1 Statistical results

Figure 8 shows scatter plots of measured and estimated from COARE 3.0 bulk algorithm [7] near surface fluxes including all the data points and measured neutral transfer coefficients against wind speed at 10 m reference height. The solid line in the scatter plots is the equality line and bulk algorithm predictions are shown by solid or dashed lines in the neutral transfer coefficients plots. The latter plots were produced
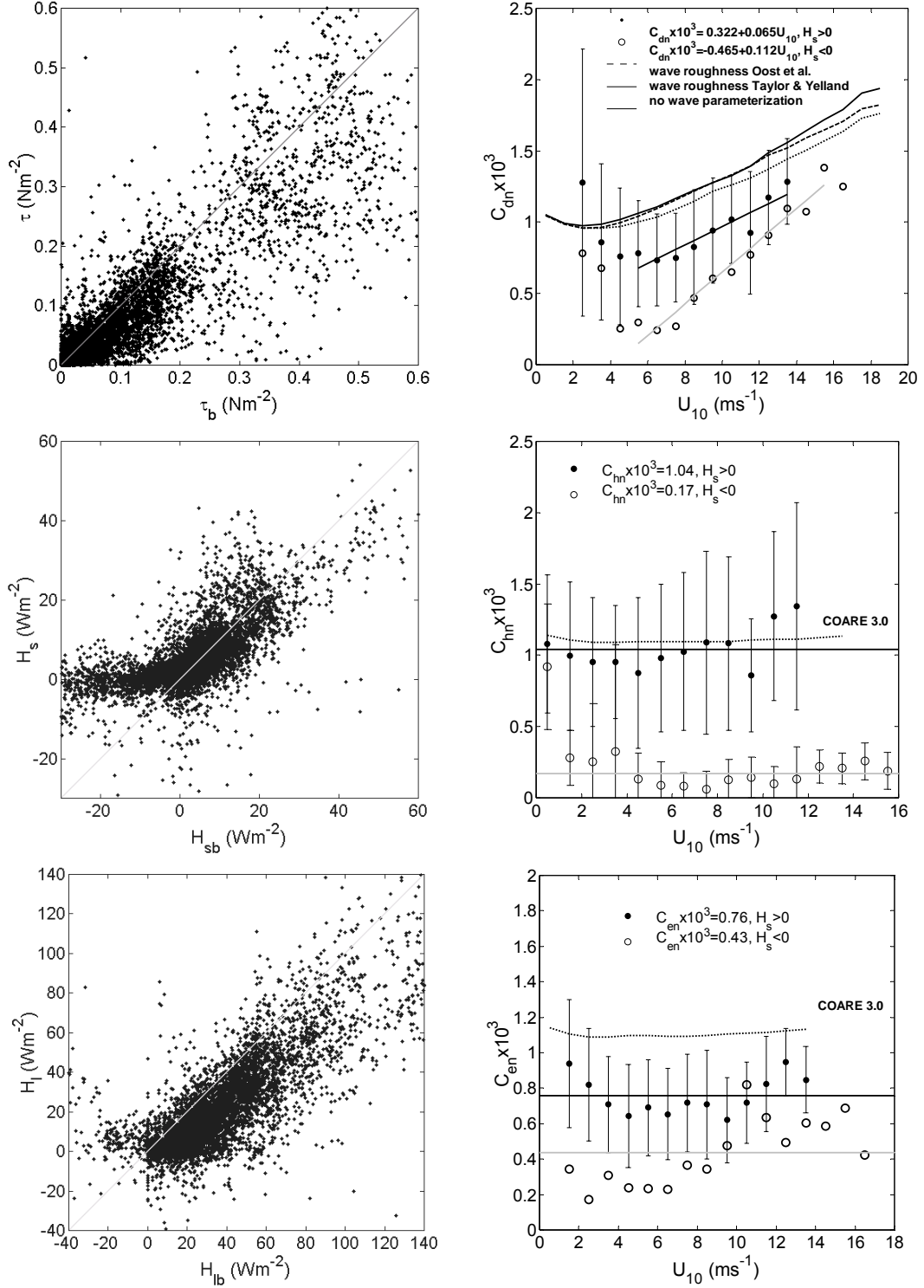
FIG. 8. Scatter plots of measured turbulence fluxes against ones estimated with a bulk method and measured neutral transfer coefficients against wind speed U_{10} at 10 m reference height. Subscript *b* indicates bulk estimate and subscript *n* indicates neutral conditions.

9

with bin averaging of data in wind speed bins of 1 ms^{-1}. The standard deviation of the corresponding coefficient in each bin is also shown. The majority of flux values are small (below 0.2 Nm^{-2} for stress, 30 Wm^{-2} for H_s and 60 Wm^{-2} for H_l) as expected due to the small stability z/L values. It is clear that stress and latent heat fluxes are systematically overestimated by the bulk algorithm. Bulk estimates of sensible heat flux predict well on average the measured values for positive values (unstable conditions) but fail under stable conditions where measurements indicate smaller values than the bulk algorithm. Similar results have been reported by other researchers [8,11] for a different areas of the California coast and for a limited dataset. Note that we use sensible heat flux instead of buoyancy flux that includes water vapor flux in the categorization of data in 'stable' (H_s<0) and 'unstable' (H_s>0) atmospheric conditions because in this section we are studying transfer coefficients of sensible and latent heat fluxes.

Further insight of the differences between measured and bulk estimated fluxes is provided from the analysis of neutral transfer coefficients in Fig. 8. We note that the COARE profile functions were used for the conversion to neutral conditions but the conversion effect is small due to small z/L values. Transfer coefficients plotted against wind speed exhibit a great deal of scatter which is believed to be the consequence of the large number of processes that are taking place in the surface layer above the sea like the effect of swell [10] and their effect on turbulence fluxes has not been resolved accurately yet. Many investigations [14,15,16,17] have demonstrated that additional scaling parameters like wave age are required to describe turbulent variables within the wave boundary layer. Measured neutral transfer coefficients are lower than bulk algorithm prediction except the coefficient for the sensible heat flux as the comparison of fluxes indicated. The neutral transfer coefficient for momentum shows an increase with increasing wind speed as found by other researcher [6,7,18,19] and an increase at low wind speed due to viscous effects. The effect of sea surface waves on roughness length was included with parameterizations (based on wave age or wave steepness) used in COARE algorithm which seem to improve but not significantly the bulk stress estimates. We note that dominant wavelength and time period of waves were estimated from wind speed as described in [7] using formulas for fully developed sea which maybe not the case for wind blowing from the land (short fetch). A significant feature of neutral transfer coefficients is that for stable atmospheric conditions they are significantly lower than the values for unstable conditions similar to the results of [9,10].

The flux divergence between sea surface and the measurement height due to the inhomogeneity of the flow in the coastal region and a possible bias in sea surface radiometric measurement could be factors that contribute to the observed discrepancies. We estimated the flux divergence from the equations for mean wind speed components, temperature and water vapor mixing ratio [20] assuming static conditions. The horizontal gradient terms were estimated after an interpolation of measured quantities near sea surface on a regular grid with 5 km spacing and then differentiation. The dense horizontal sampling permits these calculations, while the vertical gradients are multiplied with vertical velocity, thus, their effect is expected to be small and can be ignored or surface similarity functions may be used to get an approximate value of these terms. It should be noted that if measurements are within surface layer flux divergence is close to zero and the horizontal non-homogeneity (advection effect) leads to non-stationary conditions. Thus, the flux divergence correction should be used with caution. The bias error of sea surface temperature measurement was estimated to be about 0.5 ^{o}K using the assumption that the sensible heat flux H_s value should approach zero as the difference (θ_s-θ) approaches zero. The results after applying these corrections are shown in Fig. 9. The neutral transfer coefficient for momentum is now closer to the bulk estimates for moderate and high wind speed and there is no significant difference between stable and unstable conditions values. At low wind speeds the measurement error is significant due to the small values of wind stress and, thus, the sensitivity of the transfer coefficient estimation to the correction for flux gives quite high values of the transfer coefficient. The neutral transfer coefficients for sensible and latent heat fluxes were corrected only for sea surface measurement bias. Their corrected values have similar behavior as expected due to the fact that heat and mass are transported by molecular diffusion near the sea surface, while momentum can be transported also by pressure forces on the roughness elements [6,18,21]. However, both coefficients are still lower than bulk estimates and the difference due to stability remains with average values of about 0.7x10^{-3} and 0.2x10^{-3} for unstable and stable atmospheric conditions, respectively, and a small change with wind speed.

Figure 10 shows scatter plots measurements of neutral transfer coefficient for sensible heat flux C_{hn} and correlation of air temperature and water vapor mixing ratio versus wind speed with the restrictions that |H_s|>2 Wm^{-2} and |θ_s-θ|>0.5 ^{o}K in order to exclude measurements with significant measurement
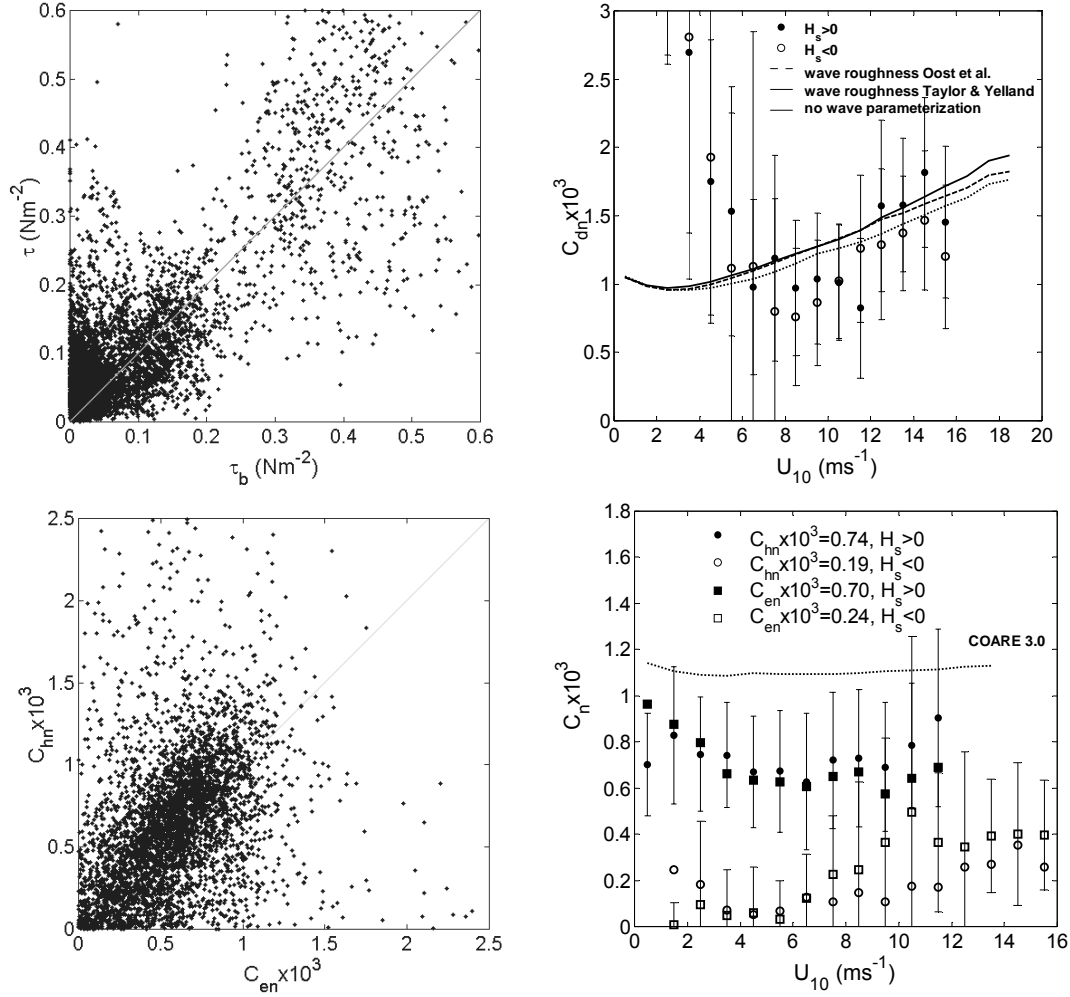
FIG. 9. Same as Fig. 8 but with turbulence fluxes corrected for vertical divergence (momentum) and bias of sea surface temperature measurement (heat).
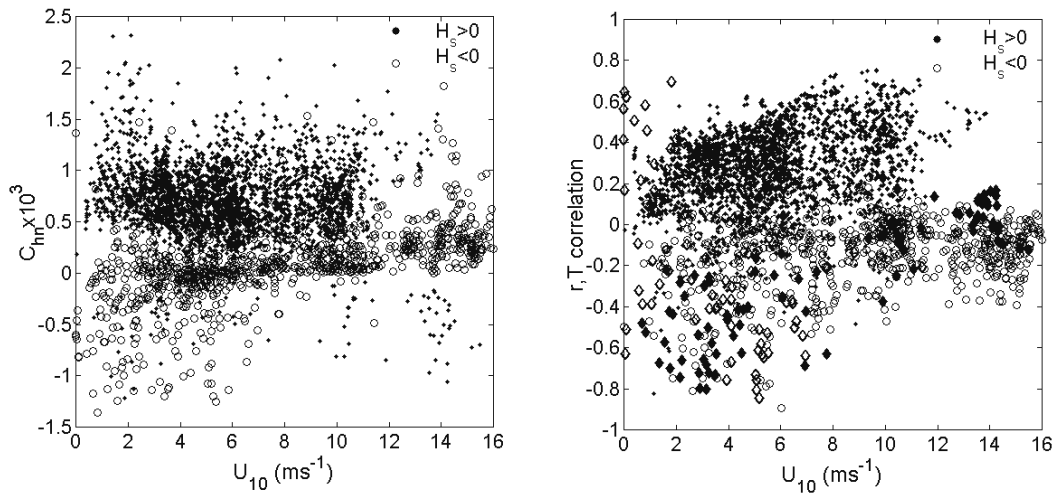

FIG. 10. Scatter plots of neutral transfer coefficient for sensible heat flux and correlation of air temperature T and water vapor mixing ratio r versus wind speed at 10 m reference height. Diamonds in the correlation plot indicate negative C_{hn} values.

relative errors. This figure shows the existence of negative values of C_{hn} (that is, opposite signs of H_s and $\theta_s-\theta$) for small H_s and both stable and unstable atmospheric conditions. Negative values of C_{hn} have been also observed for unstable atmospheric conditions by other researchers [9] with low Bowen ratios (as observed also here) and were attributed to possible water condensation at a height between sea surface and measurements height. According to Fig. 10 negative C_{hn} values and $H_s>0$ have a correlation of air temperature and water vapor mixing ratio that increases from negative values at low wind speed to positive values at high wind speed. The opposite trend (positive correlation at low winds to negative correlation at moderate winds) occurs for $H_s<0$ cases. Thus, it is possible that different mechanisms give the observed negative C_{hn} values under stable or unstable conditions. We note that the effect of sea spray evaporation, which enhances sensible and latent heat fluxes near sea surface, is more significant with increasing wind speed [22,23] and this may be linked with the observed trend of the correlation of air temperature and water vapor.

4.2 Spatial distribution

Figure 11 shows spatial distribution of measured and bulk estimated neutral transfer coefficients. The bulk estimated transfer coefficients were estimated from wind stress without correction for flux divergence. They have a pattern similar with wind speed in Fig. 1 because they increase with wind speed (especially C_{dn}) as seen in Figs. 8 and 9. The measured C_{dn} pattern has lower values towards the coastline which is parallel to the wind speed (similar with wind stress) and higher values offshore and at the coastline that is facing the wind (around Monterey peninsula). This general pattern suggests that C_{dn} and, thus, the velocity roughness length may be strongly connected with the sea surface wave field which is expected to be more well-developed at the coastline with alongshore wind and, thus, has larger wave age and lower C_{dn} values [6,17]. This pattern is locally disturbed by the presence of local wind speed maximum and
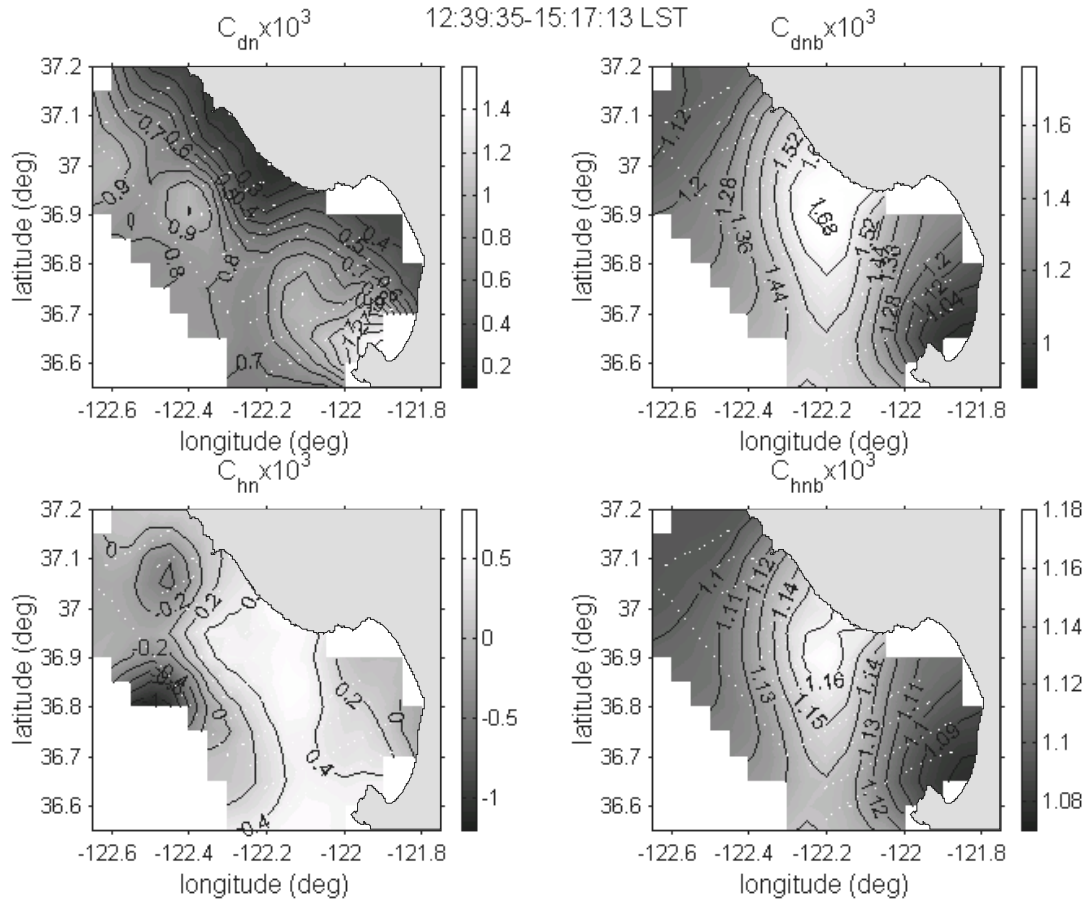

FIG. 11. Neutral momentum and sensible heat flux transfer coefficients on 13 July 2003.

negative heat flux in the area of the expansion fan. The pattern of measured C_{hn} shows a more significant increase at the wind speed maximum compared to the bulk estimate but with lower values in accordance with Figs. 8 and 9 for $H_s < 0$. The maximum of measured C_{hn} occurs at this area as the corresponding bulk estimates. At the west part of the flight area the sensible heat flux has small negative values and measured C_{hn} becomes negative. It should be noted that at this part of the flight area there were low level clouds which are expected to affect significantly the sensible heat flux though the mechanism of condensation or evaporation of water droplets. The clouds disappeared at the east part of the flight area because of the subsidence in the expansion fan discussed in section 3.1.
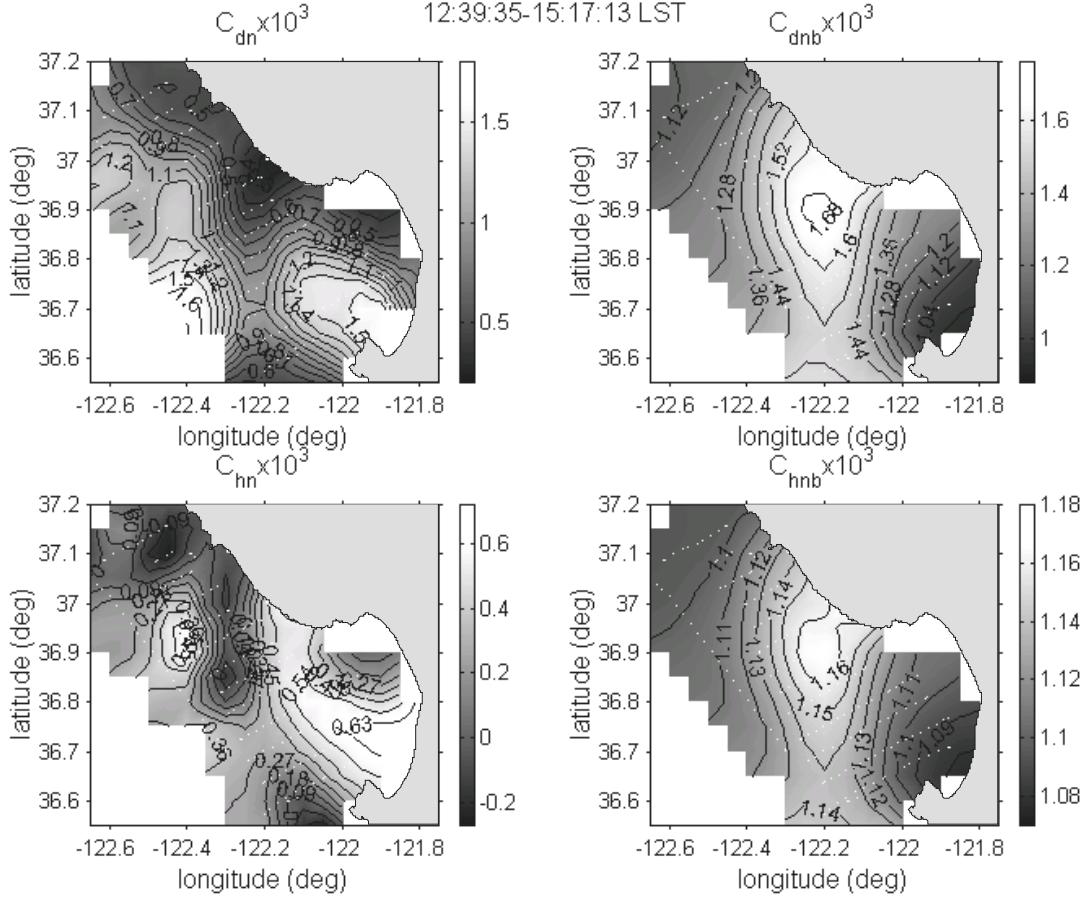

FIG. 12. Same as Fig. 11 but for turbulence fluxes corrected for vertical flux divergence.

The spatial distribution of neutral transfer coefficients estimated from turbulence fluxes corrected for flux divergence shown in Fig. 12 is different from Fig. 11. This is especially true for the case of C_{hn} which now has a spatial distribution that resembles the spatial distribution of C_{dn}, something that is not observed in Fig. 11. Also, the angle between wind and corrected wind stress reaches values up to 60 degrees (not shown here) which could be the result of significant direction shear (wind stress should be aligned with wind shear and not wind speed) on that specific experimental day. It should be noted that the spatial distribution of the measured neutral drag coefficients C_{dn} on that day (even when corrected for flux divergence) does not resemble the bulk estimate as Fig. 9 implies on average for the full data set. Thus, the behavior of transfer coefficients in each case can be very different from the average behavior because physical factors like wave effects and in-homogeneity that are not parameterized correctly or at all contribute significantly to the observed variability (scatter) of transfer coefficients.

5. CONCLUSIONS

The results of this work show that in the area of Monterey Bay characteristic local flow patterns occur under different synoptic conditions. However, minor differences in synoptic conditions like wind direction and strength and large scale subsidence may result in different small scale flow pattern. The reason for this sensitivity is probably the complexity of interaction of the atmosphere with coastal topography, sea water upwelling and the existence of low stratocumulus cloud. Interesting features like southerly surges and flow channeling were observed and could be the subject of further analysis.

The analysis of near surface turbulence fluxes showed that surface similarity functions used in bulk parameterizations of surface fluxes may not be valid in a complex coastal environment. Low values compared to bulk parameterization and different behavior of transfer coefficients under unstable and stable cases was observed. The most obvious characteristic of a wind disturbed water surface that could contribute to these observations is the complex and ever changing pattern of surface waves that makes difficult the correct parameterization of wave roughness. Additionally, wave breaking alters the surface and adjacent boundary layers in fundamental ways by introducing spray into the atmospheric boundary layer which directly changes sensible and latent heat fluxes near sea surface. However, the differences of observed transfer coefficients and estimated by the bulk algorithm are too large to explain by possible effects of wave field alone.

Advection effects in the non-homogeneous environment of measurements area should also be significant especially under stable conditions when the boundary layer adjusts slowly to changes of the surface forcing (sea surface temperature). Furthermore, the wave field reacts slower than boundary layer turbulence in changes of the wind speed and, thus, wave age and wave induced roughness vary with local changes of wind speed. Flux divergence correction and sea surface temperature bias could be significant factor in the accuracy of the results using aircraft data. The correction for sea surface temperature bias was found to give same average values of transfer coefficient for sensible and latent heat fluxes, but the flux divergence correction gave ambiguous. This should be expected if measurements are actually in the surface layer and, thus, flux divergence is actually close to zero and the effects of horizontal gradients contribute to non-stationarity of the atmospheric state.

Considering the large number of processes that are taking place in the surface layer above the sea it is not surprising that measured drag coefficient exhibit great deviations from bulk estimations. The spatial variability of transfer coefficients showed that wave age and cloud effects could be factors that contribute more to this discrepancy. Aircraft measurements of cloud and wave parameters (like radar wave spectrometers), which were not available in the present study, would be quite valuable in understanding the behavior of near sea surface turbulence, supplement similarity theory and improve surface fluxes parameterizations.

REFERENCES

[1] Enriquez, A.G., and C.A. Friehe, 1995: Effects of wind stress and wind stress curl variability on coastal upwelling. *J. Phys. Oceanogr.*, **25**, 1651-1671.

[2] Zemba, J., and C.A. Friehe, 1987: The marine atmospheric boundary layer jet in the Coastal Ocean Dynamics Experiment. *J. Geophys. Res.*, **92** (C2), 1489-1496.

[3] Burk, S. D., and W.T. Thompson, 1996: The summertime low-level jet and marine boundary layer structure along the California coast. *Mon. Wea. Rev.*, **124**, 668-686.

[4] Winant, C.D., C.E. Dorman, C.A. Friehe and R.C. Beardsley, 1988: The marine layer off the northern California: An example of supercritical flow. *J. Atmos. Sci.*, **45**, 3588-3605.

[5] Banta, R.M., L.D. Olivier, and D.H. Levinson, 1993: Evolution of the Monterey Bay sea-breeze layer as observed by pulsed Doppler Lidar. *J. Atmos. Sci.*, **50**, 3959-3982.

[6] Enriquez, A.G., and C.A. Friehe, 1997: Bulk parameterization of momentum, heat, and moisture fluxes over a coastal upwelling area. *J. Geophys. Res.* **102**, *C3*, 5781-5798.

[7] Fairall, C.W., Bradley, E.F., Hare, J.E., Grachev, A.A., and J.B. Edson, 2003: Bulk parameterization of air-sea fluxes: Updates and verification for COARE algorithm. *J. Climate*, **16**, 571-591.

[8] Rogers, D.P., Dorman, C.E., Edwards, K.A., Brooks, I.M., Melville, W.K., Burk. S.D., Thompson, W.T., Holt, T., Ström, L.M., Tjernström, M., Grisogono, B., Bane, J.M., Nuss., W.A., Morley, B.C., and A.J. Schanot, 1998: Highlights of Coastal Waves 1996. *Bull. Amer. Meteor. Soc.*, **79**, *7*, 1307-1326.

[9] Oost, W.A., C.M.J. Jacobs and C. Van Oort, 2000: Stability Effects of Heat and Moisture Fluxes at sea, *Bound.-Layer Meteor.*, **95**, 271-302.

[10] Rutgersson, A., A. Smedman, and U. Högström, 2001: The use of conventional stability parameters during swell, *J. Geophys. Res.,* **106**, 27,117– 27,134.

[11] Brooks, I.M., Södergberg, S., and M. Tjernström, 2001: The turbulence structure of the stable atmospheric boundary layer around a coastal headland: I. Aircraft observations. *Preprints:* 4th *Conference on Coastal Atmospheric and Oceanic Prediction and Processes*, AMS Boston, 37-42.

[12] Kalogiros, J.A., and Q. Wang, 2002: Calibration of a radome-differential GPS system on a Twin Otter research aircraft for turbulence measurements, *J. Atmos. Oceanic Technol.*, **19**, 159-171.

[13] F. M. Ralph, L. Armi, J. M. Bane, C. Dorman, W. D. Neff, P. J. Neiman, W. Nuss and P. O. G. Persson, 1998: Observations and Analysis of the 10–11 June 1994 Coastally Trapped Disturbance. *Mon. Wea. Rev.*, **126**, 2435–2465.

[14] Geernaert, G. L., K. B. Katsaros, and K. Richter, 1986: Variation of the drag coefficient and its dependence on sea state. *J. Geophys. Res.,* **91***,* 7667-7679.

[15] Donelan, M.A., F.W. Dobson, S.D. Smith, and R.J. Anderson, 1993: On the dependence of sea surface roughness on wave development. *J. Phys. Oceanogr.,* **23**, 2143-2149.

[16] Hare, J.E., T. Hara, J.B. Edson, and J.M. Wilczak, 1997: A similarity analysis of the structure of air flow over surface waves. *J. Phys. Oceanogr.,* **27**, 1018-1037.

[17] Drennan, W.M., H.C. Graber, D. Hauser, and C. Quentin, 2003: On the wave age dependence pf wind stress over pure wind seas. *J. Geophys. Res.,* **108***, 8062-8074.*

[18] Garrat, J.R., 1992: *The Atmospheric Boundary Layer*. Cambridge University Press, 316 pp.

[19] Large, W. G., and S. Pond, 1981: Open ocean momentum flux measurements in moderate to strong winds. *J. Phys. Oceanogr.*, **11**, 324-336.

[20] Stull, R.B., 1988: *An Introduction to Boundary Layer Meteorology*. Kluwer Academic Publishers, 666 pp.

[21] Liu, W.T., K.B. Katsaros, and J.A. Businger, 1979: Bulk parameterization of air-sea exchanges of heat and water vapor including the molecular constraints at the interface, *J. Atmos. Sci.*, **36**, 1722-1735.

[22] DeCosmo, J., K. B. Katsaros, S. D. Smith, R. J. Anderson, W. A. Oost, K. Bumke and H. Chadwick, 1996: Air-sea exchange of water vapor and sensible heat: The Humidity Exchange over the Sea (HEXOS) results. *J. Geophys. Res.*, **101**, 12,001-12,016.

[23] Andreas, E. L., and J. DeCosmo, 1999: Sea spray production and influence on air-sea heat and moisture fluxes over the open ocean. *Air-Sea Exchange: Physics, Chemistry and Dynamic*s, G. L. Geernaert, Ed., Kluwer, 327–362.